


Comparison of regenerative braking technologies for heavy goods vehicles in urban environments

Proc IMechE Part D:
J Automobile Engineering
0(0) 1–14
© IMechE 2012
Reprints and permissions:
sagepub.co.uk/journalsPermissions.nav
DOI: 10.1177/0954407011433395
pid.sagepub.com


William JB Midgley and David Cebon

Abstract

One way to reduce the carbon dioxide emissions of heavy vehicles is to install regenerative braking systems. These capture the kinetic energy of the vehicle during braking and store it, in order to feed it back into the drivetrain during acceleration. It is not clear, however, which of the many available technologies should be used to implement this regenerative braking.

This report explores the different possible energy capture and storage technologies for regenerative braking, including electrical, kinetic, hydraulic and compressed air. The basic systems are plotted on a selection chart, and an optimal selection methodology is used to aid in the selection of the lightest and smallest system for regenerative braking.

The results of this comparison and selection show that hydraulic energy storage is likely to be 33% smaller and 20% lighter than the closest electrical counterparts and is therefore a logical selection for regenerative braking on the trailers of heavy goods vehicles.

Keywords

Regenerative braking, energy storage, hybrid vehicle, heavy vehicle, hydraulic hybrid

Date received: 13 May 2011; accepted: 24 November 2011

Introduction

In 2008, road transport was responsible for 23% of the UK's carbon dioxide (CO₂) emissions¹ and transport fuels accounted for 67% of the UK's oil demand.² Heavy goods vehicles (HGVs) travelled 28.7×10^9 km; 16% of these were on urban roads.³ At least 3.6×10^6 t of CO₂ were produced by HGVs in urban areas in 2008.^{3,4}

A study conducted by Odhams et al.⁵ concluded that urban delivery would be up to 25% more fuel efficient with articulated trucks than with rigid trucks, and up to an additional 20–30% more fuel efficient if these articulated trucks featured regenerative braking (depending on the drive cycle). (This is primarily due to the increased freight capacity of an articulated vehicle, which leads to a higher ratio of payload mass to unladen mass of the vehicle. In addition, the aerodynamic drag per unit mass of payload is lower for an articulated vehicle than for a rigid vehicle.)

Other emissions studies have shown up to 30% increase in fuel economy for hybrid vehicles.^{7–11} Thus a very effective way to reduce the emissions from HGVs in urban delivery would be to use articulated HGVs with regenerative braking in the place of traditional

rigid vehicles. These measures are more effective than others available (Table 1). Such vehicles may need to incorporate steered axles on the trailer so as to have sufficient manoeuvrability.⁶

To make use of such a regenerative braking system, and to provide an acceptable braking performance for the HGV, the system must be fitted to all axles on the vehicle; otherwise insufficient tyre friction is available to stop the vehicle. In this analysis it is assumed that the system can be segmented, with the trailer and tractor having different and self-sufficient regenerative braking systems.

Several different technologies can be used to implement hybridisation and each of these is discussed in turn in the second section. Companies such as Volvo have made electric hybrid tractor units,^{7,8} Eaton makes both electric and hydraulic hybrid propulsion systems for heavy vehicles,^{9–11,13,14} and Permo-Drive (an

Department of Engineering, University of Cambridge, UK

Corresponding author:

David Cebon, Department of Engineering, University of Cambridge, Trumpington Street, Cambridge CB2 1PZ, UK.
Email: dc@eng.cam.ac.uk

Table 1. Comparison of fuel usage reduction measures.

Fuel usage reduction measure	Approximate reduction (%) in the fuel consumption per freight task ^a	Reference
Articulated vehicles	25	Odhams et al. ⁵
Regenerative braking	20	Odhams et al. ⁵
Stop-start hybrid	7	Baker et al. ¹²
Aerodynamic improvements	7	Baker et al. ¹²
Tyre improvements	7	Baker et al. ¹²
Engine efficiency improvements	3	Baker et al. ¹²

^aRelative to the baseline tractor–semitrailer.

Australian company) makes a hydraulic hybrid drive for heavy vehicles.^{15,16} This paper will focus on regenerative braking on the trailer, as there are several systems already developed (see above) for a driven vehicle.

Each technology has advantages and disadvantages. No thorough comparison of hybrid technologies is available in the current literature, and so this paper aims to establish which technology is best for implementation of regenerative braking on the trailer of an articulated urban delivery vehicle.

Component technologies

Existing technologies for regenerative braking include electric, kinetic (e.g. flywheels) and hydraulic energy storage. Details of these technologies were gathered from manufacturers' data sheets; these sources are included in Table 2 and Table 3. The main comparison metrics used in this paper are the specific energy, the specific maximum power, the volumetric energy and the volumetric maximum power, where a *specific property* is defined as the amount of that property per unit mass, and a *volumetric property* is the amount of that property per unit volume.

Electric hybrids

Background. In an electric hybrid vehicle, energy is normally stored either in a battery or in an electric double-layer capacitor (often known as an 'ultra-capacitor').⁵⁵ A battery stores energy chemically, whereas a capacitor (or ultra-capacitor) stores energy through charge separation. Batteries tend to have high specific energies, while capacitors have comparatively higher specific powers and lower specific energies.^{56,57} These devices are used to store energy recovered from regenerative braking or to store any extra power generated by the vehicle's powerplant. Electric motor–generators are used as the transformers between the rotational motion and the electrical energy. Several manufacturers, including Volvo, use this technology for hybrid heavy vehicles.^{7,9}

Table 2. Sources of energy storage specifications.

Storage device	Information source		
Battery	AI23 Systems ANR26650M1A ¹⁷		
	Panasonic CGA103450A ¹⁸ CGR26650A ¹⁹		
	Energizer NH12-850 ²⁰ NH50-2500 ²¹ NH22-175 ²²		
	Oak Ridge National Laboratory Toyota Prius battery pack ^{23,24}		
	Tesla Motors Inc. Tesla battery pack ^{25,26}		
	Continental Automotive ²⁷ LF4-60 ELF2-60 ELFI-1		
	Ultra-capacitor	Maxwell Technologies Inc. BCAP0350 ²⁸ BMOD0063 ²⁹ BCAP3000 ³⁰	
		Metal accumulator	HYDAC GmbH ³¹ 10 l bladder 50 l bladder 0.6 l diaphragm Eaton Hydraulics Corporation ³² A2 50 578 A2 50 15G A2 30 060 A2 30 578
			Composite accumulator
	Flywheel		ULEV-TAP 2 project ³⁷ IEEE review of flywheels ³⁸
	Elastomer		Research by Hoppie ³⁹

Batteries. Batteries are often operated in a small fraction of their total energy storage range (some only between 55% and 60% of the state of charge (SOC)⁵⁸) because of large excursions from optimal charging and discharging efficiencies, and also to prolong the service life of the battery. As a result, numerous methods for managing the SOC of the batteries have been suggested.^{59–65}

Data describing several commercially available 'state-of-the-art' electrical energy storage devices were collected (see Table 2), and the relevant comparison metrics (specific and volumetric powers and specific and volumetric energies) were calculated.

The faster a battery is discharged, the greater the energy dissipated across the internal resistance, and therefore the lower the energy available at the terminals of the battery.⁶⁶ An example discharge curve is given in Figure 1. Consequently, the energy storage of each battery was calculated from data given in the product data sheet at a discharge rating of '0.5C' which corresponds to a 2 h discharge time. This means that, if a battery is rated at 125 mA h, the discharge curve corresponding to 62.5 mA is used to calculate the total energy stored. The 0.5C rating was used as it is normally a good point

Table 3. Sources of actuator specifications.

Actuation device	Information source		
Electric motor-generator	Oak Ridge National Laboratory Toyota Prius electric motor-generator ^{23,24}		
	UQM Technologies Inc. Powerphase 75 ⁴⁰ Powerphase 100 ⁴¹ Powerphase 150 ⁴²		
	Moog Motors ⁴³ Moog BN42 53IP Moog BN23-28EU Moog D326 HT		
	Bosch Rexroth Ltd Bosch 24 V 1.7 kW ⁴⁴ Bosch 12 V 1.6 kW ⁴⁵		
	Hydraulic pump-motor	Bosch Rexroth Ltd ^{46,47} Rexroth A4VSG 40 Rexroth A4VSG 180 Rexroth A4VSG 750 AA4 CSG 250 AA4 CSG 750	
		Eaton Hydraulics Corporation ⁴⁸ ADU041 ADU062	
		CVT	Novel rolling traction CVT ⁴⁹ NASA review of CVTs ⁵⁰ Next-generation toroidal CVT ⁵¹
			Air-powered motors

CVT: continuously variable transmission.

on the discharge curve of most rechargeable batteries, corresponding to a nominal 2 h discharge time. This is a generous concession to batteries, especially in regenerative braking systems, as the charge and discharge times can be much faster (of the order of seconds rather than hours).

As discussed above, electric hybrid systems often use a narrow band of the battery's total SOC range in order to prolong the battery life and to avoid inefficient charging and discharging regimes.^{58,60,67} These values vary widely, with some academic studies using a range of only 10% of the SOC,⁵⁸ while other academic studies use a range of up to 60% of the SOC.^{68,69} This information is not available from manufacturers. A representative factor of 50% of the SOC was applied to the energy storage capacities quoted in or calculated from the batteries' data sheets.

In existing commercial hybrid electric vehicles the battery packs are formed by combining many small single-cell batteries. For example the battery pack in

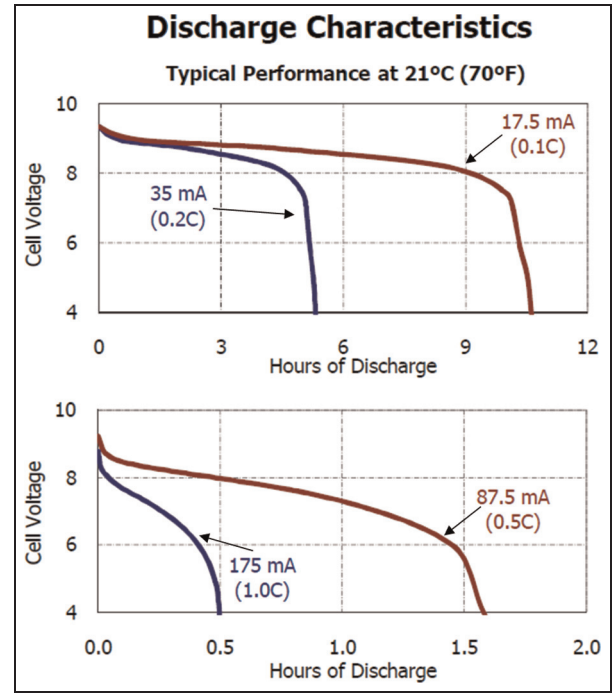


Figure 1. Discharge curves for an energizer NH22-I75.²²

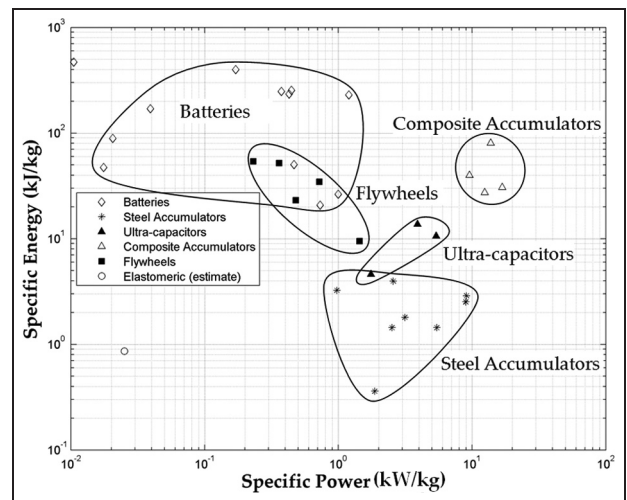


Figure 2. Storage device comparison chart: specific properties.

the Tesla Roadster uses 6831 batteries, each slightly larger than an AA battery and with a nominal voltage of 3.7 V,^{25,26} and the Toyota Prius uses 28 battery modules each with a nominal voltage of 7.2 V.⁷⁰

These battery packs require cooling (and heating) in order to keep them at an optimal temperature for operation. Additionally they require complex inter-cell energy management in order to spread the load across the cells.²⁵ These complications add to the mass and complexity of an electrical hybrid.

The specific energies and specific powers of a number of suitable batteries¹⁷⁻²⁷ are plotted in Figure 2. The volumetric energies and powers are plotted in Figure 3.

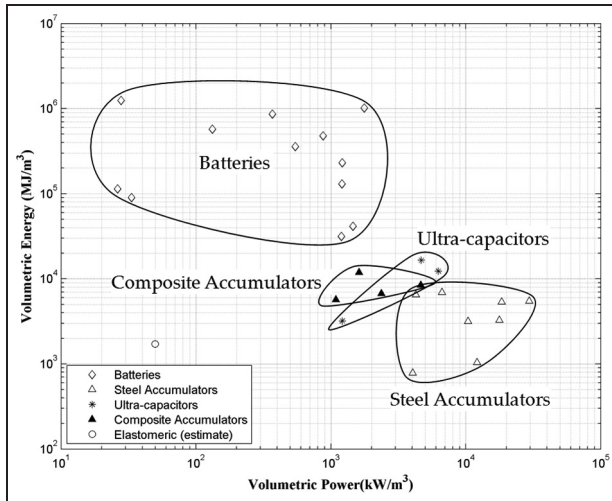


Figure 3. Storage device comparison chart: volumetric properties.

Ultra-capacitors. Data for ultra-capacitors are generally given in the manufacturer's data sheets; alternatively the stored energy U can be calculated using $U = \frac{1}{2}CV^2$, where C is the capacitance of the ultra-capacitor and V is the voltage across its terminals. Ultra-capacitors suffer from similar SOC concerns to batteries, primarily because of the difficulty of extracting energy from them at low voltages. Only 75% of the energy stored in an ultra-capacitor is used;^{68,71} therefore, a factor of 75% was applied to the energy storage capacities quoted in the ultra-capacitors' data sheets. The properties of several ultra-capacitors from Maxwell Technologies Inc.^{28–30} are plotted in Figure 2 and Figure 3.

Batteries and ultra-capacitors are sometimes combined in order to take advantage of the benefits of each of them.^{56,57,72} The ultra-capacitor is used to serve large power demands, and the battery to store larger quantities of electrical energy. The two devices are joined by a d.c.-to-d.c. converter and complex power electronics.

When a battery and an ultra-capacitor are joined together, it is possible to calculate the properties of the combination when the fraction x of energy E_u stored by the ultra-capacitor is varied in relation to the amount of energy E_b stored in the battery according to

$$\frac{E_u}{E_b} = x \quad (1)$$

The total energy E_t stored by the combination is then

$$\begin{aligned} E_t &= E_u + E_b \\ &= E_b(1 + x) \end{aligned} \quad (2)$$

The specific energy of a battery–ultra-capacitor combination e_t is then given by

$$\begin{aligned} e_t &= \frac{E_b(1 + x)}{m_u + m_b} \\ &= \frac{e_b(1 + x)}{1 + xe_b/e_u} \end{aligned} \quad (3)$$

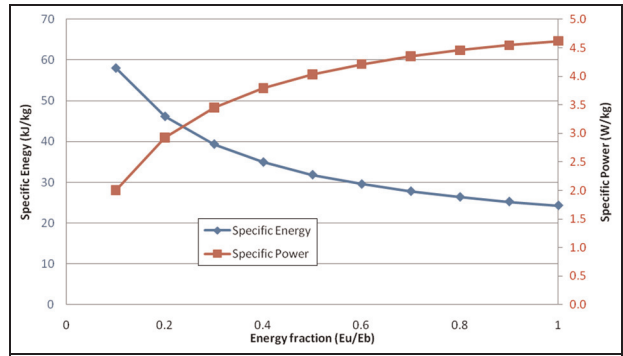


Figure 4. The effect of varying the energy fraction on a battery–ultra-capacitor combination.

where e_b and e_u are the specific energies (energy per unit mass) of the battery and the ultra-capacitor respectively, and m_u and m_b are the masses of the ultra-capacitor and the battery respectively.

The specific power (power per unit mass) \dot{e}_t of the combination is governed by the power \dot{E}_u of the ultra-capacitor, as these can accept higher power rates than batteries, and is given by

$$\begin{aligned} \dot{e}_t &= \frac{\dot{E}_u}{m_b + m_u} \\ &= \frac{\dot{e}_u}{1 + e_u/e_b x} \end{aligned} \quad (4)$$

An illustration of the results of a battery–ultra-capacitor combination (in this case, using the battery from a Toyota Prius and a Maxwell BCAP3000 ultra-capacitor) is shown in Figure 4, where the x axis is the fraction x discussed above. Figure 4 shows that, as the capacity of the ultra-capacitor is increased to equal that of the battery (towards the right of the x axis), the specific power of the combination increases, but the specific energy decreases. The optimal point in this range depends on the nature of the application, and the relative importance of the specific energy compared with the specific power.

Kinetic hybrids

Kinetic hybrids store energy in the form of kinetic energy using flywheels and a continuously variable transmission (CVT) to transfer energy between the flywheel and the drivetrain. Defining a system as purely electric or purely kinetic can be misleading, especially if the drivetrain is electrical but the energy is stored in a flywheel rather than a battery or ultra-capacitor. This storage method is typically called a 'flywheel battery'.

The energy E_f that a flywheel stores is related to the rotational speed ω of the flywheel and the rotational inertia J of the flywheel according to

$$E_f = \frac{1}{2}J\omega^2 \quad (5)$$

To maximise E_f it is desirable to spin the flywheel as fast as the limits of the material will allow. The top speed ω_{max} is limited by the fracture stress σ_f of the material. Equating the centrifugal stress at the centre of a spinning disc to the failure stress gives an expression for the maximum speed in terms of the density ρ and the radius R of the flywheel⁷³ according to

$$\omega_{max}^2 = \frac{2\sigma_f}{\rho R^2} \quad (6)$$

Modern composite materials have a high specific ultimate strength σ_f/ρ MPa/m³/kg, which allows much higher rotational speeds and therefore higher stored energy.⁷⁴ Consequently, flywheels have become more popular as a means of storing energy.

In order to minimise losses from windage (the effect of the aerodynamic drag on the rotating surface of the flywheel), the flywheels are often housed in a vacuum. In order to stop mechanical losses through friction, high-energy flywheels may use electromagnetic bearings in the place of traditional roller bearings.⁷⁵

In 1988, Vint and Gilmore⁷⁶ designed and built a prototype bus that coupled hydraulics with a flywheel storage system and predicted a fuel saving of around 20% for a suburban cycle. Instead of using a CVT or electric motor-generator to speed up and/or to slow down the flywheel, a variable-displacement hydraulic pump-motor was used. This final design was expected to have a pay-back period of between 4 years and 10 years.

In 1997 a study by Wicks and Donnelly⁷⁷ suggested that an idealised mechanical flywheel could give potential fuel savings of up to 59% for a city bus. This calculation used an average in-service drive cycle for the bus.

For the 2009 Formula One racing season the Fédération Internationale de l'Automobile⁷⁸ allowed teams to add kinetic energy recovery systems (KERSs) to their cars. The Williams Formula One team^{79,80} developed an innovative flywheel concept for this purpose, in which the rotor of the flywheel is built from a magnetically doped composite. This enables the flywheel to act as both an energy storage device and an integrated motor-generator. Other companies such as Bosch and Flybrid Systems Inc. have designed CVT-based flywheels for Formula One.^{81,82} A flywheel KERS has yet to be used in a Formula One championship race. (KERSs were only available to teams in the 2009 Formula One season, and the only systems that were used in championship races were those which used batteries.)

The data on the flywheels from the work of Henning et al.³⁷ and Hebner et al.³⁸ are plotted in Figure 2 and Figure 3.

Hydraulic hybrids

In hydraulic accumulators, energy is stored in the compression of a gas (usually nitrogen) by hydraulic fluid. The fluid is separated from the gas by a bladder, a diaphragm or a piston. As fluid is pumped into one side of the accumulator, the gas is compressed.⁸³

Hydraulic hybrid vehicles use two hydraulic accumulators: one at a high pressure and one at a low pressure. During regenerative braking, a hydraulic pump-motor takes torque from the wheels or drivetrain and pumps fluid from the low-pressure accumulator to the high-pressure accumulator. To remove this energy from the system the pump-motor is used as a motor, transferring fluid from the high-pressure accumulator to the low-pressure accumulator and producing a torque. Eaton¹⁴ and Permo-Drive¹⁵ use embodiments of this technology for implementing a regenerative braking system on hybrid heavy vehicles.

The energy stored E_{acc} in an accumulator can be calculated assuming adiabatic compression of the nitrogen⁸⁴ from

$$E_{acc} = \left[P_{comp} \frac{1 - r_v^{1-\gamma}}{\gamma - 1} - P_{atm}(r_v - 1) \right] v_{comp} \quad (7)$$

where P_{comp} is the pressure of the gas in its compressed state, r_v is the volumetric compression ratio, γ is the adiabatic index (approximately 1.4 for nitrogen), P_{atm} is the atmospheric pressure and v_{comp} is the volume of the gas in its compressed state.

Adiabatic compression is more representative of the process inside an accumulator than isothermal compression is, as the temperature of the working fluid (nitrogen) will increase during the compression process.⁸⁵ Heat can be lost through the walls of the accumulator, but thermal insulation on the 'gas side' (i.e. the part of the vessel in contact with the gas) can reduce these losses.⁸⁶ Both Pourmovahed and Otis⁸⁵ and Wu et al.⁸⁶ clearly demonstrated that using thermal insulation foam on the gas side of the accumulator (in order to minimise thermal losses) reduced the losses in the accumulator dramatically.

The specific energy (energy per unit mass) of hydraulic systems depends strongly on the mass of the accumulators. Conventional accumulators are made from steel; however, pressure vessels for transport operations are increasingly made from lighter composite materials, and this option was considered worthy of investigation. Both composite pressure vessels and ultra-capacitors are emerging technologies, and only one manufacturer could be found for each.

The instantaneous power flow into or out of the accumulator is $\dot{E}_{acc} = PQ$ where P is the pressure and Q is the flow rate. Both the pressure and the flow rate vary non-linearly during a typical stop. Consequently, the average power was calculated from half the maximum flow multiplied by the pressure halfway through the range of pressures according to

$$\begin{aligned} \dot{E}_{avg} &= Q_{avg} \frac{P_{max} + P_{min}}{2} \\ &= \frac{Q_{max}}{2} P_{max} \frac{1 + P_{min}/P_{max}}{2} \\ &= Q_{max} P_{max} \frac{1 + 1/r_p}{4} \end{aligned} \quad (8)$$

$$\dot{E}_{avg} = Q_{max} P_{max} \frac{r_p + 1}{4r_p} \quad (9)$$

where \dot{E}_{avg} is the average power of the accumulator and r_p is the pressure ratio of the accumulator (the ratio of the maximum working pressure to the minimum working pressure).

For a stop with a constant braking torque, it is clear that the average power dissipated by the vehicle is half the maximum, because the decrease in the rotational speed of the wheels is linear. It is less obvious that the average accumulator power is half the maximum flow rate multiplied by the average pressure in the accumulator. However, this has been confirmed as a valid assumption by comparing the average powers from equation (9) with those obtained from a mathematical model of the thermodynamics of the accumulator.⁸⁷

The benefits of hydraulic energy storage in a series hydraulic hybrid were investigated in 1985 by Wu et al.⁸⁶ It was concluded that the efficiencies of the hydraulic components were 'key to the system's fuel efficiency', and that a 1360 kg car might attain 60 miles/gal over the US Federal Urban Drive Cycle. A practical investigation (i.e. charging and discharging the accumulator) by Pourmovahed et al.^{88,89} suggests that the 'round-trip' efficiencies in a hydraulic regenerative braking system may vary between 61% and 89% on a simple stop-start test. This efficiency depends heavily on the angle of the swash plate in the hydraulic pump-motor.

In hydraulic pump-motors, the hydraulic fluid is used to rotate components either through restriction of the flow (as in a gear pump) or by actuation of the pistons by the hydraulic fluid (as in a swash plate pump).

Variable pump-motors are typically based on the swash plate and piston principle; altering the angle of the swash plate changes the net displacement of each of the pistons over a full cycle. This in turn changes the amount of torque provided by the motor, or the amount of fluid delivered by the pump.

At low rotational speeds (below 500 r/min) the efficiencies of variable pump-motors become low.⁹⁰ This means that, in order to use them to drive vehicle wheels efficiently, they need to be geared through a ratio of approximately 1:8. Using product data sheets it was estimated that, even if pump-motors are engaged for low-speed take-off (0–8 miles/h or 0–3.6 m/s), then the additional losses would amount to 5% of the stored energy. Therefore the system can be run at low speeds with small losses, and multiple gear ratios (in order to 'step up' the low-speed operating points) should not be needed. If these losses are too high, then the pump-motor could be idled for this inefficient part of the cycle and engaged at an appropriate speed.

Artemis Intelligent Power has converted a BMW 5 series sedan into a series hydraulic hybrid using their patented digital displacement pumps.^{91,92} This hybrid used approximately 34% less fuel on the US Combined Drive Cycle than the original unmodified BMW 5 series does.

A series hybrid suggested by Innas BV uses an internal combustion engine to drive a fixed-displacement pump, which then drives an innovative 'hydraulic transformer' to pump fluid from one accumulator to the other.^{93–95} Another hydraulic transformer then acts as a CVT between the accumulators and the fixed-displacement wheel motors. This configuration removes the mechanical drivetrain completely⁹³ and so provides the torque directly to the wheels.

Hydraulic systems have also had limited use in delivery vehicles; Wu et al.⁹⁶ simulated a parallel hydraulic regenerative braking system and quoted fuel economy increases of 28–47% on the Federal Urban Drive Schedule (FUDS) drive cycle, and UPS are currently testing a small fleet of hydraulic hybrids in the USA.⁹⁷ Additionally, a study by Filipi et al.⁹⁸ showed fuel economy improvements of 32% for a parallel 6 × 6 medium tactical truck over a custom-designed drive cycle. However, a study by Toulson⁹⁹ suggested that, for smaller road vehicles, fuel savings of only 7–10% are achievable over the Urban Dynamometer Drive Schedule and the Supplemental Federal Test Procedure (both American drive cycles).

The specific energies and powers for steel accumulators^{31,32} and for composite accumulators^{33–36} are plotted in Figure 2. The volumetric powers and energies are plotted in Figure 3.

Other technologies

Other technologies such as elastomeric and compressed air energy storage were also explored. Elastomeric regenerative braking was studied by Hoppie³⁹ in 1983. He investigated the viability of using elastomers to store energy when coupled with a clutch. However, the system was not able to provide a variable torque and so would require coupling to a CVT. In addition, the volumetric energy of the elastomer was 0.29 kW h/m³, less than that of a lithium-ion battery. Data points corresponding to the estimated properties of Hoppie's experimental set-up are included in Figure 3 and Figure 2. These properties were estimated using the average density of elastomers and the estimated size of the final experimental set-up.

A study by Wicks et al.¹⁰⁰ proposed using air compression as a means of regenerative braking. Heating this air with the exhaust from the vehicle could double the effectiveness of this technique; however, it is admitted that the stopping time required for this heating is longer than a typical stopping time. Other technologies exist which use compressed air to provide the motive force for the vehicle.¹⁰¹ The properties for compressed-air storage are plotted in Figures 2 and 3.

Note on efficiencies

Mechanical, electrical and hydraulic systems all have high efficiencies of the order of 90–95%, but these vary with the details of the design. Efficiencies are

difficult to quantify without manufacturing and testing the hardware. However, the differences between systems are relatively small in comparison with the other issues described above. Consequently, for comparison purposes, the inefficiencies in all systems have been ignored.

System plotting and selection

Creating and plotting plausible solutions

A regenerative braking system must combine an energy storage device with an actuator and, in order to compare these systems, a method was needed to specify each system. This was achieved by a power-matching argument: the power of the actuator was matched with the power of the energy storage device. Power matching of components implies that the storage device will be able to accept energy at the rate at which the actuator can supply it during braking, and vice versa under acceleration.

The specific power \dot{e}_s of energy storage and the specific power \dot{e}_a of the actuators (motors) are calculated from

$$\begin{aligned}\dot{e}_s &= \frac{\dot{E}_s}{m_s} \\ \dot{e}_a &= \frac{\dot{E}_a}{m_a}\end{aligned}\quad (10)$$

where \dot{E}_s is the power of the energy storage, \dot{E}_a is the power of the actuator and m_s and m_a are the masses of the storage and actuator respectively.

It is necessary to have sufficient storage to accept all the power developed by the actuator. This can be achieved by matching their powers according to

$$\begin{aligned}\dot{E}_s &= \dot{E}_a \\ \dot{e}_s m_s &= \dot{e}_a m_a\end{aligned}\quad (11)$$

In order to find the specific power \dot{e}_t of the entire system, the power of the system which is given by $\dot{E}_t = \dot{E}_a = \dot{E}_s$ is divided by its mass m_t according to

$$\dot{e}_t = \frac{\dot{E}_t}{m_t} = \frac{\dot{e}_s m_s}{m_a + m_s} = \frac{\dot{e}_a m_a}{m_a + m_s}\quad (12)$$

(In this case the mass of the system is taken to be the mass of the storage system plus the mass of the actuator. This does not take into account the mass of the piping and pipe fittings (hydraulics) or the mass of the power electronics (electrical) as this would require an in-depth specification. It does, however, take account of the fluid in the hydraulic system.) Using equation (11) this gives

$$\dot{e}_t = \frac{1}{1/\dot{e}_a + 1/\dot{e}_s} = \frac{\dot{e}_s}{1 + \dot{e}_s/\dot{e}_a}\quad (13)$$

In a similar fashion the specific energy e_t of the system can be obtained from

$$e_t = \frac{E_t}{m_t} = \frac{e_s}{1 + \dot{e}_s/\dot{e}_a}\quad (14)$$

From equation (13), it is clear that the specific power of the system is increased if the specific power of either the storage device or the actuator is increased. Increasing the specific power of either component decreases its mass for a specified duty and consequently decreases the mass of the system. From equation (14) it is clear that, as the specific energy of the storage device is increased, so is the specific energy of the system, for the same reason.

Equations similar to equations (13) and (14) can be obtained for volumetric power $\dot{\tilde{e}}_t$ and volumetric energy \tilde{e}_t according to

$$\dot{\tilde{e}}_t = \frac{\dot{\tilde{e}}_a}{1 + \dot{\tilde{e}}_a/\dot{\tilde{e}}_s}\quad (15)$$

$$\tilde{e}_t = \frac{\tilde{e}_s}{1 + \dot{\tilde{e}}_s/\dot{\tilde{e}}_a}\quad (16)$$

An important assumption in this analysis is that the hydraulic motor, air motor and electric motor are geared using one stage and therefore do not require an additional gearbox or CVT. It is also assumed that this one stage is sufficient to overcome any angular velocity constraints and that the actuator can be decoupled from the wheels if necessary (e.g. to prevent the actuator from going over its maximum angular velocity). If a full gearbox were required, then the mass of this gearbox would have to be included in the analysis. Based on the analysis in the second section and existing systems such as the Volvo delivery truck^{7,8} and the Eaton hydraulic hybrid vehicle,¹⁴ this assumption is considered to be reasonable. By definition, the kinetic and elastomeric energy storage methods require a CVT in order to transmit the torque from the flywheel to the wheels. In this case the ‘actuator’ for a kinetic system was taken to be the CVT, and account was taken of the driveshaft used for the torque transmission.

Implicit in this calculation is the idea that existing storage and actuation devices may not be exactly the correct size for the particular application. However, it is assumed that existing commercial devices can be scaled up or down while maintaining the same specific and volumetric energies and specific and volumetric powers. This may not be precisely true but is thought to be a reasonable approximation since the devices included in the analysis were all in a reasonable size range for this application.

MATLAB was used to create a matrix of all possible power-matched combinations of components (one energy storage device with one actuation device), keeping the systems entirely hydraulic, entirely electric or entirely kinetic. (Air motors were power matched with accumulators, and elastomeric storage was power matched with a CVT.) These combinations were plotted on axes where each point on the chart corresponds to a plausible solution in the technology space. Each chart combines two decision metrics; either specific or volumetric properties, with energy on the y axis and with power on the x axis. These charts are shown in Figures

5 and 6, with ovals showing rough technology groupings. (Note that no kinetic (flywheel–CVT) systems are shown in Figures 6 and 8 because volume data were not available for CVTs.^{49–51})

The curves in Figures 5, 6, 7 and 8 correspond to battery–ultra-capacitor combinations, with the parameter x varying from 0.1 to 1. These curves demonstrate how the presence of the ultra-capacitor can increase the specific and volumetric powers of the combination at the expense of decreased specific and volumetric energies.

It is often the case that systems look as though they are grouped along a curve or are close together. This is especially evident in Figure 6. These groupings correspond to a specific energy storage device coupled with a number of different actuators.

Selection criteria

In general, it is desirable to minimise the mass and volume of the system for any given power or energy specification (towards the top right-hand corner of

each of the charts in Figures 7 and 8). However, it is not clear exactly where on these charts the best solutions for this particular application lie.

In order to minimise the mass of the system it is necessary to size the components so that the design is ‘balanced’, i.e. it is not over-designed for either the power or the energy requirement. This can be achieved by ensuring that the system mass $m_{t,p}$ needed to meet the maximum power demand is equal to the system mass $m_{t,e}$ needed to meet the energy storage demand as given by

$$m_{t,p} = m_{t,e} \tag{17}$$

Using equation (10) this becomes

$$\frac{\dot{E}_{max}}{\dot{e}_t} = \frac{E_v^0}{e_t} \tag{18}$$

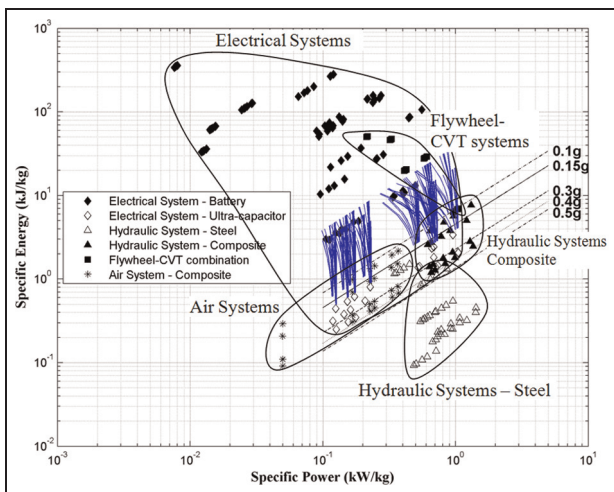


Figure 5. System selection chart: specific properties. CVT: continuously variable transmission.

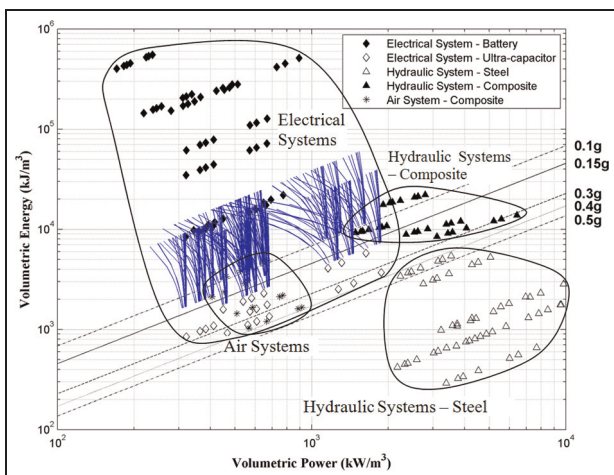


Figure 6. System selection chart: volumetric properties.

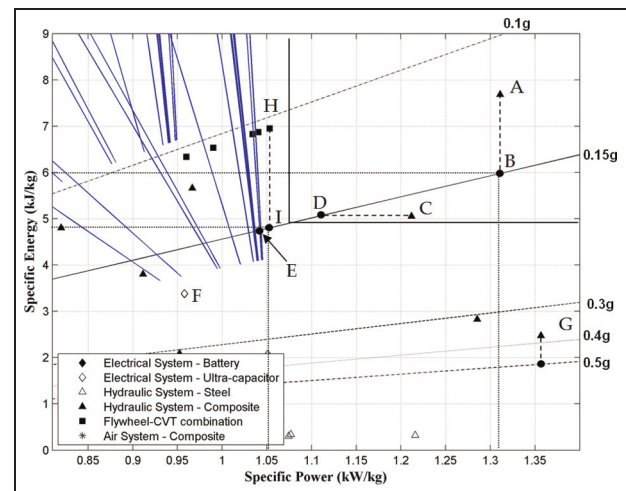


Figure 7. Magnified section of the system selection chart: specific properties (linear scale). CVT: continuously variable transmission.

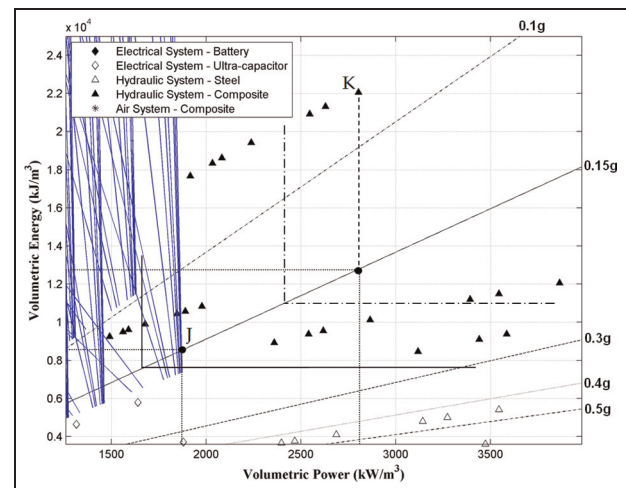


Figure 8. Magnified section of the system selection chart: volumetric properties (linear scale).

where E_v^0 is the energy to be stored (the vehicle's kinetic energy at the beginning of the stop), e_t and \dot{e}_t are the specific energy storage and the maximum specific power respectively of the regenerative braking system and \dot{E}_{max} is the maximum power dissipated by the decelerating vehicle.

If the mass of the vehicle is m_v , its initial velocity is v_i and the demanded deceleration is a_d , then

$$E_v^0 = \frac{1}{2} m_v v_i^2 \quad (19)$$

$$\dot{E}_{max} = m_v a_d v_i \quad (20)$$

Substituting equations (19) and (20) into equation (18) gives

$$e_t = \frac{v_i}{2a_d} \dot{e}_t \quad (21)$$

Equation (21) is plotted in Figure 5 for an initial vehicle speed $v_i = 30$ miles/h = 13.4 m/s and various values of a_d . This gives a set of parallel lines of slope 1 on the log-log graph.

A similar derivation applies for the volumetric energy and power (energy and power per unit volume). In this case the system volumes needed to meet the energy and power requirements must be equated and the result is

$$\tilde{e}_t = \frac{v_i}{2a_d} \dot{\tilde{e}}_t \quad (22)$$

A set of lines corresponding to equation (22) with an initial vehicle speed $v_i = 30$ miles/h = 13.4 m/s and various values of a_d is plotted in Figure 6.

In both Figure 7 and Figure 8 the most desirable system is the lightest or the smallest system, while still fulfilling the required criteria: power matching, storing the energy from the stop and accepting the energy at the rate demanded by the desired deceleration rate.

Figures 7 and 8 show the best-performing systems from Figures 5 and 6, this time plotted on linear scales. This means that the lines corresponding to equation (21) and equation (22) now have different gradients.

Use of the selection line

The selection line enables a rigorous definition of the best point in the technology space by representing the direct trade-off between each of the properties on the x and y axes. The best system on one of these charts for, say, a 0.15 g stop is that furthest along the 0.15 g selection line, towards the top right corner of the chart.

Systems that do not lie on a selection line are only as good as equivalent systems located by 'projecting' their position on to the line. For example, in Figure 7, for a 0.15 g stop the system labelled A is only as good as a system located at point B. This is because the mass of the system needed to absorb the power at B is significantly greater than the mass needed to store the energy for the system at A. Therefore, if the mass were chosen to store the necessary energy, the system would be too

small to accept the full power; i.e. the system is 'over-specified' for energy; its specific energy performance is better than it needs to be for a 0.15 g stop.

Similarly the system located at position C in Figure 7 is no better than the system located at D. The system at C is over-specified for power. In order to store sufficient energy it would need to have a higher mass than is necessary to absorb the power.

The best-performing system in Figure 7, i.e. the lowest mass system for, say, a 0.15 g stop, is the hydraulic system with a composite accumulator, located at A. The nearest electrical system, at E, is a combination battery-ultra-capacitor system with a battery-ultra-capacitor fraction of $x = 0.75$. This system would have a mass of 26% more for the same duty. The closest single storage type of electric system (an ultra-capacitor system) at point F would have a mass of 77% more than the hydraulic system at A. In fact, the system at A is best for all decelerations less than 0.4 g . However, for a 0.4 g or 0.5 g stop, the hydraulic system at G would be best. The closest competing system to the hydraulic system at A is the kinetic system at point H. This would have a performance equivalent to a system at I and would be 17% heavier than the hydraulic system at A.

An alternative way to view this is by moving the corner of the selection area defined by the lines which meet at a right angle on the selection line. For example, in Figure 8, if the corner is moved up past the best combination electrical system at point J ($x = 0.75$) on the selection line, this system will no longer be within the selection area, but many hydraulic systems will be. Thus the hydraulic systems are the better choice. The hydraulic system at point K would have a 33% lower volume than the nearest equivalent electrical system at J.

These charts show that hydraulic regenerative braking systems are preferable to electric or kinetic systems when specific and volumetric properties are used as the decision metrics. Hydraulic systems are up to 33% smaller and 20% lighter than the nearest equivalent electrical systems.

Further considerations

While this paper has focused on the practical considerations of the size and mass of a regenerative braking system for the trailer of an HGV, there are several other factors to be considered when selecting a technology. These include (but are not limited to) cost; controllability, packaging and duty cycle. Each of these will be briefly discussed below.

System costs, safety and durability

Cost is a significant factor to take into account when designing and building a regenerative braking system, especially for urban delivery vehicles. The profit margins in freight transport are low (typically 2–3%) and so a project has to have a short payback period

(typically 6–8 months). Hydraulic systems have a significantly lower cost than electrical or kinetic alternatives because of their simplicity and small number of components, most of which are available ‘off the shelf’ at low cost. Hydraulic systems have been in widespread use for many decades, and many of the processes and parts are as simple and cost effective as possible. They use readily available low-cost materials.

Wear within hydraulic systems is low, provided that standard precautions are taken to keep the hydraulic fluid clean. Oil leaks are rare in properly designed systems. There are risks associated with the storage of pressurised hydraulic fluid. ‘Flow fuses’ and pressure-relief valves can be used to mitigate the risks posed by a system failure.

Analogous risks and safety precautions exist for kinetic and electrical systems. Electrical systems use high voltages (typically around 300 V) and high currents to drive the electric machines. These voltages must be properly managed with fuses and controller logic in order to minimise the risk of electric shock. The battery packs must also be closely managed in order to ensure that each battery stays within its recommended limits. These risks can be managed with a sufficiently well-designed battery pack and controller.

Kinetic energy storage also poses a risk. If a flywheel delaminates (the outer part separates from the inner part), then there is a risk that high-velocity particles injure a bystander. Covering a flywheel in a blast shield can help to reduce the risk that this occurs; however, it adds substantially to the mass of the system.

The durability of each of the systems is an ongoing area of research. Hydraulic systems are likely to be very durable; seal changes in the motors and filtering–degassing of the fluid are likely to be the main in-service requirements for longevity. Electric systems are perhaps more durable; however, the battery pack will have to be replaced regularly (usually after 3 years). In kinetic systems, the main problem is wear in the bearings on the flywheel due to the high rotational speeds.

Controllability

Several aspects of the controllability of a hydraulic regenerative braking system have been discussed in a previous paper,¹⁰² which concludes that variable-displacement pump–motors are the best choice for ensuring controllability of the hydraulic regenerative braking system. However, with appropriate design trade-offs, fixed-displacement pumps could also be used. These are smaller and simpler and cost less than variable-displacement pumps.

Packaging

As this regenerative braking system is envisaged for installation on an HGV, packaging is not as constrictive as it may be in a passenger car. There is a large amount of room underneath the trailer of an HGV, where the

under-run guards are currently placed. However, it is still better to choose a regenerative braking system which occupies minimal volume, as a larger system may have to take up space within the cargo area of the HGV.

This system is designed for urban delivery cycles and so it is unlikely that the vehicle will be ‘massed out’ (at its maximum tare mass); it is far more likely to be ‘cubed out’ (volumetrically filled). The additional mass of the regenerative braking system will increase the total mass of the vehicle but may not impact upon the carrying capacity of the vehicle. However, if the regenerative braking system is too heavy, it will start to reduce the amount of freight that the vehicle can carry, making the system less beneficial.

Hydraulic pump–motors can be manufactured as in-wheel units, meaning that no drivetrain needs to be installed, further lowering the relative mass added by the hydraulic regenerative braking system. In-wheel units such as the Poclair MFE-08 series¹⁰³ can freewheel when not in use, removing the need for a clutch. If an electric motor were to be used for this application, the motor would have to be mounted in-board, with a drivetrain linking the motor to the wheels, with all the added complication of the differential and mechanical linkages.

Both the flexibility with the mass and the flexibility with the positioning of the regenerative braking system mean that the solutions for an urban HGV are not necessarily the same as those for a traditional passenger vehicle.

Duty cycle

Urban HGVs are often single-purpose vehicles, and therefore their duty cycles can be well characterised. For example, it is simpler to design a representative duty cycle for a refuse truck than for a ‘typical’ passenger car. This makes it easier to design a regenerative braking system that operates within these parameters and also makes it easier to optimise this design.

As this paper is concerned with urban HGVs undergoing typical cycles such as delivery and refuse collection, the simple cycle described in the third section above is sufficient for selection in this context. If this technology were to be developed for a different duty cycle (e.g. an extra-urban cycle involving hills), then it is likely that a different selection line would be used, and this would alter the components selected for the task.

Conclusions

A systematic methodology was devised for optimal selection of regenerative braking systems for HGVs in urban environments. This involves power matching between actuator and energy storage, as well as balancing the power and energy performance requirements for particular stopping parameters.

Hydraulic systems present the best solution for regenerative braking of HGVs, because they have their better specific power and specific energy than electrical

or kinetic systems do. Hydraulic systems are likely to be 20% lighter and 33% smaller than competing electrical technologies and 16% lighter than a flywheel-based system. In addition to these quantitative measures, a hydraulic system is competitive on cost and packaging for the chosen urban duty cycle.

The next step in this research is to create a computer model of a hydraulic regenerative braking system and, using the existing model of the Cambridge Vehicle Dynamics Consortium HGV, to predict the system's possible fuel savings over a simple stop-start cycle. This model will then be run over several standard drive cycles to characterise further the possible fuel savings of this regenerative braking system. Should the benefits prove sufficient, a prototype system will be developed to test the concept.

Funding

This work was supported by the New Zealand Foundation for Research, Science and Technology (grant no. CAMX0801) and by the Cambridge Vehicle Dynamics Consortium.

Acknowledgements

The authors would like to thank Team MRO for their help with this research. Additionally, none of this research would have been possible without the technical support of the Cambridge Vehicle Dynamics Consortium, whose members at the time of writing were as follows: ArvinMeritor, Camcon, Denby Transport, Firestone Industrial Products, Fluid Power Design, FM Engineering, Fruehauf, Goodyear, Haldex, Intec Dynamics, Mektronika Systems, MIRA, Poclairn Hydraulics, QinetiQ, Shell UK, Tinsley Bridge and Volvo Trucks.

References

1. *Digest of United Kingdom energy statistics 2009*. London: Department for Business Enterprise and Regulatory Reform, 2009.
2. *UK energy in brief 2009*. London: Department for Business Enterprise and Regulatory Reform, 2009.
3. *Road statistics 2008: traffic, speeds and congestion*. London: Department for Transport, 2009.
4. *Guidelines to Defra/DECC's greenhouse gas conversion factors for company reporting*. London: Department for Environment Food and Rural Affairs, 2009.
5. Odhams AMC, Roebuck RL, Lee YJ, et al. Factors influencing the energy consumption of road freight transport. *Proc IMechE Part C: J Mechanical Engineering Science* 2010; 224(9): 1995–2010.
6. Odhams AMC, Roebuck RL, Jujnovich BA, et al. Active steering of a tractor semitrailer. *Proc IMechE Part D: J Automobile Engineering* 2011; 225(7): 847–869.
7. *Volvo FE hybrid for distribution and refuse collection*. Göteborg: Volvo Truck Corporation, 2008.
8. Hybrid refuse trucks with regenerative braking boost fuel efficiency. *Prof Engng* 2008; 21: 51.
9. EauClaire M. Joining forces. *OEM Off-Highway* 2008; 23: 40–47.
10. Siuru Jr BD. Technology brake-through. *Waste Age* 2005; 36: 22.
11. Ehrenman G. Look, Ma, no transmission. *Mech Engng* 2005; 127: 24–26.
12. Baker H, Cornwell R, Koehler E and Patterson J. Review of low carbon technologies for heavy goods vehicles. Report for the Department for Transport, Ricardo, Shoreham-by-Sea, UK, 2009.
13. US Environmental Protection Agency. World's first full hydraulic hybrid SUV, <http://www.epa.gov/otaq/technology/420f04019.pdf> (2004, accessed 14 February 2012).
14. Wiebusch B. Hydraulic regenerative braking improves large-truck fuel economy. *Des News* 2002; 58: 69–70.
15. Permo-Drive. The hybrid solution for urban commercial vehicles. The technology, <http://permodrive.com/tech/index.htm> (2009, accessed 29 July 2009).
16. Matheson P and Stecki J. Development and simulation of a hydraulic-hybrid powertrain for use in commercial heavy vehicles. In: *International truck and bus meeting and exhibition*, Fort Worth, TX, USA, 2003, paper no. 2003-01-3370. Warrendale, PA: Society of Automotive Engineers.
17. A123 Systems. A123 ANR26650M1A product data sheet, http://www.akukeskus.ee/anr26650m1a_datasheet_april_2009.pdf (2009, accessed 14 February 2012).
18. Panasonic. CGA103450A product data sheet, http://www.panasonic.com/industrial/includes/pdf/Panasonic_LiIon_CGA103450A.pdf (2009, accessed 14 February 2012).
19. Panasonic. CGR26650A product data sheet, http://ancoobattery.com/pdf/Panasonic/Lithium/Panasonic_LiIon_CGR26650A.pdf (2009, accessed 14 February 2012).
20. Energizer. NH12-850 product data sheet, <http://data.energizer.com/PDFs/nh12-850.pdf> (2009, accessed 10 July 2009).
21. Energizer. NH50-2500 product data sheet, <http://data.energizer.com/PDFs/NH50-2500.pdf> (2009, accessed 10 July 2009).
22. Energizer. NH22-175 product data sheet, <http://data.energizer.com/PDFs/nh22-175.pdf> (2009, accessed 10 July 2009).
23. Staunton RH, Ayers CW, Chiasson JN, et al. Evaluation of 2004 Toyota Prius hybrid electric drive system. Report ORNL/TM-2006/423, Oak Ridge National Laboratory, Oak Ridge, Tennessee, USA, May 2006.
24. Hsu JS, Ayers CW, Coomer CL, et al. Toyota Prius motor torque capability, torque property, no-load back EMF, and mechanical losses. Report ORNL/TM-2004/185, Oak Ridge National Laboratory, Oak Ridge, TN, USA, September 2004.
25. Berdichevsky G, Kelty K, Straubel J and Toomre E. The Tesla Roadster battery system. Report, Tesla Motors Inc., Palo Alto, CA, USA, 2006.
26. Tesla Motors Inc. Tesla Roadster performance specifications, http://www.teslamotors.com/performance/perf_specs.php (2009, accessed 11 August 2009).
27. Continental Automotive. Battery data presentation, http://www.elektroniknet.de/fileadmin/user_upload/pdf/Batterie_2009/Session_1/05_Bronold_Continental.pdf (2009, accessed 20 August 2009).

28. Maxwell Technologies Inc. Maxwell BCAP0350 product data sheet, http://www.maxwell.com/products/ultra-capacitors/docs/DATASHEET_BC_SERIES_1017105.PDF (2009, accessed 14 February 2012).
29. Maxwell Technologies Inc. Maxwell BMOD0063 product data sheet, http://www.maxwell.com/products/ultra-capacitors/docs/DATASHEET_BMOD0063_1014696.PDF (2009, accessed 14 February 2012).
30. Maxwell Technologies Inc. Maxwell BCAP3000 product data sheet, http://www.maxwell.com/products/ultra-capacitors/docs/DATASHEET_K2_SERIES_1015370.PDF (2009, accessed 14 February 2012).
31. HYDAC GmbH. Accumulator data sheets, <http://www.hydac.com/de-en/products/hydraulic-accumulators/bladder-accumulators.html> (2009, accessed 20 July 2009).
32. Eaton Hydraulics Corporation. Accumulator data sheet, <http://hydraulics.eaton.com/products/pdfs/V-FIFIMC003-E.pdf> (2009, accessed 21 June 2009).
33. Tam WH, Drey MD, Jackson AC, et al. Design and manufacture of the ETS VIII composite overwrapped xenon pressure vessel. In: *26th international electric propulsion conference*, Kitakyusyu, Japan, 17–21 October 1999, paper no. IEC-99-244. Tokyo: Japan Society for Aeronautical and Space Sciences.
34. Tam WH, Ballinger IA, Kuo J, et al. Design and manufacture of a composite overwrapped xenon conical pressure vessel. In: *32nd AIAA/ASME/SAE/ASEE joint propulsion conference*, Lake Buena Vista, FL, USA, 1–3 July 1996, paper no. AIAA 96-2752. Reston, VA: American Institute of Aeronautics and Astronautics.
35. Kawahara G and McClesky SF. Titanium lined, carbon composite overwrapped pressure vessel. In: *32nd AIAA/ASME/SAE/ASEE joint propulsion conference*, Lake Buena Vista, FL, USA, 1–3 July 1996, paper no. AIAA 96-2751. Reston, VA: American Institute of Aeronautics and Astronautics.
36. Grimes-Ledesma L, Phoenix SL, Beeson H, et al. Testing of carbon fiber composite overwrapped pressure vessel stress-rupture lifetime. In: *ASC/ASTM 21st annual technical conference of the American Society for Composites*, Dearborn, MI, USA, 17–20 September 2006, paper no. 06-1957. Pasadena, CA: NASA.
37. Henning U, Thoelen F, Lamperth M, et al. Ultra low emission traction drive system for hybrid light rail vehicles. In: *International symposium on power electronics, electrical drives, automation and motion*, Taormina, Sicily, Italy, 23–26 May 2006, pp.1068–1072. Piscataway, NJ: IEEE.
38. Hebner R, Beno J and Walls A. Flywheel batteries come around again. *Spectrum, IEEE* 2002; 39: 46–51.
39. Hoppie LO. *Elastomeric regenerative braking systems*. Warrendale, PA: SAE International, 1983.
40. UQM Technologies, Inc. Powerphase 75 data sheet, http://www.et.aau.dk/digitalAssets/17/17715_uqm_powerphase_75.pdf (2009, accessed 14 February 2012).
41. UQM Technologies, Inc. Powerphase 100 data sheet, <http://www.gielow.org/PowerPhase100.pdf> (2009, accessed 14 February 2012).
42. UQM Technologies, Inc. Powerphase 150 data sheet, <http://electrotransport.ru/ussr/index.php?action=dlattach;topic=4546.0;attach=18878> (2009, accessed 14 February 2012).
43. Moog Motors. Data sheet, <http://www.polysci.com/docs/mosilencerseries.pdf> (2009, accessed 5 July 2009).
44. Bosch Rexroth Ltd. Bosch 24 V 1.7 kW data sheet, http://www2.eng.cam.ac.uk/~wjbm2/References/Bosch_24V_1.7kW.pdf (2009, accessed 14 February 2012).
45. Bosch Rexroth Ltd. Bosch 12 V 1.6 kW data sheet, http://www2.eng.cam.ac.uk/~wjbm2/References/Bosch_12V_1.6kW.pdf (2009, accessed 14 February 2012).
46. Bosch Rexroth Ltd. Variable-displacement pump A4VSG data sheet, http://www.boschrexroth.com/RDSearch/rd/r_a-92100/raa-92100_1997-10.pdf (2009, accessed 14 February 2012).
47. Bosch Rexroth Ltd. Axial piston compact unit data sheet, http://www.boschrexroth.com/country_units/america/united_states/sub_websites/brus_brh_i/en/products_ss/09_pumps/a_downloads/ra92105_0504.pdf (2009, accessed 14 February 2012).
48. Eaton Hydraulics Corporation. 420 mobile piston pump data sheets, http://www.eaton.com/ecm/idcplg?IdcService=GET_FILE&allowInterrupt=1&RevisionSelectionMethod=LatestReleased&Rendition=Primary&dDocName=DEV_216798 (2009, accessed 14 February 2012).
49. Akehurst S, Brace C, Vaughan ND, et al. Performance investigations of a novel rolling traction CVT. SAE paper 2001-01-0874, 2001.
50. Loewenthal SH, Rohn DA and Anderson NE. Advances in traction drive technology. SAE paper 831304, 1983.
51. Shinojima T, Toyoda T, Miyata S, et al. Development of the next-generation toroidal CVT-gear neutral and power-split system for 450 N m engines. *NSK Tech J* 2005; 679: 1–9.
52. *PIV-B technical catalogue*. Norwich: Parker Hydraulics, 2001.
53. *PIV-B technical catalogue*. Norwich: Parker Hydraulics, 2009.
54. Radial piston air motors. Data sheet series PIV-P, Parker Pneumatics, Norwich, UK, 2008.
55. Inman S, El-Gindy M and Haworth DC. Hybrid electric vehicles technology and simulation: literature review. *Int J Heavy Veh Systems* 2003; 10: 167–187.
56. Lu S, Corzine KA and Ferdowsi M. A new battery/ultracapacitor energy storage system design and its motor drive integration for hybrid electric vehicles. *IEEE Trans Veh Technol* 2007; 56: 1516–1523.
57. Bauman J and Kazerani M. A comparative study of fuel-cell-battery, fuel-cell-ultracapacitor, and fuel-cell-battery-ultracapacitor vehicles. *IEEE Trans Veh Technol* 2008; 57: 760–769.
58. Lin C-C, Kang J-M, Grizzle JW and Peng H. Energy management strategy for a parallel hybrid electric truck. In: *2001 American control conference*, Arlington, VA, USA, 25–27 June 2001, pp.2878–2883. New York: IEEE.
59. Lin C-C, Jeon S, Peng H and Lee JM. Driving pattern recognition for control of hybrid electric trucks. *Veh System Dynamics* 2004; 42: 41–58.
60. Lin C-C, Peng H, Jeon S and Lee JM. Control of a hybrid electric truck based on driving pattern recognition. In: *6th international symposium on advanced vehicle control*, Hiroshima, Japan, 9–13 September 2002, vol. 42, pp.41–58. Tokyo: Japan Society of Automotive Engineers.
61. Lin C-C, Peng H, Grizzle JW and Kang J-M. Power management strategy for a parallel hybrid electric truck. *IEEE Trans Control Systems Technol* 2003; 11: 839–849.

62. Cao J, Cao B, Chen W and Xu P. Neural network self-adaptive pid control for driving and regenerative braking of electric vehicle. In: *2007 IEEE international conference on automation and logistics*, Jinan, People's Republic of China, 18–21 August 2007, pp.2029–2034. New York: IEEE.
63. Cao J, Cao B, Xu P and Bai Z. Regenerative-braking sliding mode control of electric vehicle based on neural network identification. In: *IEEE/ASME international conference on advanced intelligent mechatronics*, Xian, People's Republic of China, 2–5 July 2008, pp.1219–1224. New York: IEEE.
64. Dextreit C, Hannis G, Burnham K, et al. Power management techniques for hybrid vehicles. In: *18th international conference on systems engineering* (eds KJ Burnham and OCL Haas), Coventry, UK, 5–7 September 2006. Coventry, UK: Coventry University.
65. Wang F, Zhong H, Mao X-J, et al. Regenerative braking algorithm for a parallel hybrid electric vehicle with continuously variable transmission. In: *IEEE international conference on vehicular electronics and safety*, Beijing, People's Republic of China, 13–15 December 2007, pp.1–4. New York: IEEE.
66. Kim D, Hwang S and Kim H. Vehicle stability enhancement of four-wheel-drive hybrid electric vehicle using rear motor control. *IEEE Trans Veh Technol* 2008; 57: 727–735.
67. Lin C-C, Filipi Z, Louca L, et al. Modelling and control of a medium-duty hybrid electric truck. *Intl J Heavy Veh Systems* 2004; 11: 349–371.
68. Mierlo J, Van den Bossche P and Maggetto G. Models of energy sources for EV and HEV: fuel cells, batteries, ultracapacitors, flywheels and engine-generators. *J Power Sources* 2004; 128: 76–89.
69. Van den Bossche P. *The electric vehicle: raising the standards*. PhD Thesis Natural Sciences, Vrije University, Brussels, Belgium, 2003.
70. *Toyota Prius Hybrid 2010 model 3rd generation emergency response guide*. Toyota City, Aichi: Toyota Motor Corporation, 2010.
71. Moreno J, Ortuzar ME and Dixon JW. Energy-management system for a hybrid electric vehicle, using ultracapacitors and neural networks. *IEEE Trans Ind Electron* 2006; 53: 614–623.
72. Lu S, Corzine KA and Ferdowsi M. A unique ultracapacitor direct integration scheme in multilevel motor drives for large vehicle propulsion. *IEEE Trans Veh Technol* 2007; 56: 3945–3992.
73. Ashby MF. *Materials selection in mechanical design*, 3rd edition. Oxford: Butterworth-Heinemann, 2005.
74. Castelvechi D. Spinning into control. *Sci News* 2007; 171: 312–313.
75. Ruddell A. Investigation on storage technologies for intermittent renewable energies: evaluation and recommended R&D strategy. INVESTIRE Thematic Network, Storage Technology Report WP-ST6: Flywheel, Council for the Central Laboratory of the Research Councils, Rutherford Appleton Laboratory, Chilton, Didcot, Oxfordshire, UK, 2003.
76. Vint MK and Gilmore DB. Simulation of transit bus regenerative braking systems. *Math Comput Simulation* 1988; 30: 55–61.
77. Wicks F and Donnelly K. Modeling regenerative braking and storage for vehicles. In: *32nd intersociety energy conversion engineering conference*, Honolulu, HI, 27 July–1 August 1997, vol. 3, pp.2030–2035. New York: American Institute of Chemical Engineers.
78. Formula One Administration Limited. KERS summary, http://www.formula1.com/inside_f1/understanding_the_sport/8763.html (2009, accessed 6 August 2009).
79. Williams Hybrid Power Ltd. KERS technology explained, <http://www.williamshybridpower.com/technology/whps-flywheel-technology> (2009, accessed 14 February 2012).
80. Armstrong-Wilson C. Williams F1 KERS explained, <http://www.racecar-engineering.com/articles/f1/williams-f1-kers-explained/> (2009, accessed 14 February 2012).
81. Collins S. F1 KERS: Bosch goes modular. In: *Racecar engineering*, vol. 19. London: IPC Media, 2008, pp. 65–67.
82. Armstrong-Wilson C. F1 KERS system: Flybrid, <http://www.racecar-engineering.com/news/racing-tech/f1-kers-flybrid-2/> (2008, accessed 14 February 2012).
83. Clegg SJ. A review of regenerative braking systems. Working Paper 471, Institute of Transport Studies, University of Leeds, UK, 1996.
84. Li PY, Van de Ven JD and Sancken C. Open accumulator concept for compact fluid power energy storage. In: *ASME 2007 international mechanical engineering congress and exposition*, Seattle, WA, USA, 11–15 November 2007, pp.127–140. New York: ASME.
85. Pourmovahed A and Otis DR. An experimental thermal time-constant correlation for hydraulic accumulators. *Trans ASME, J Dynamic Systems Measmt Control* 1990; 112: 116–121, 1990.
86. Wu P, Luo N, Fronczak FJ and Beachley NH. Fuel economy and operating characteristics of a hydropneumatic energy storage automobile. SAE paper 851678, 1985.
87. Midgley WJB and Cebon D. Comparison of regenerative braking technologies for heavy vehicles. Technical Report, University of Cambridge, UK, 2010.
88. Pourmovahed A, Beachley NH and Fronczak FJ. Modeling of a hydraulic energy regeneration system: Part II – experimental program. *Trans ASME, J Dynamic Systems Measmt Control* 1992; 114: 160–165.
89. Pourmovahed A, Beachley NH and Fronczak FJ. Modeling of a hydraulic energy regeneration system: Part I – analytical treatment. *Trans ASME, J Dynamic Systems Measmt Control* 1992; 114: 155–159.
90. *Vickers PVM piston pumps – technical data*. Eden Prairie, MN: Eaton Hydraulics Corporation, 2009.
91. Ehsan M, Rampen WHS and Salter SH. Modeling of digital-displacement pump-motors and their application as hydraulic drives for nonuniform loads. *Trans ASME, J Dynamic Systems Measmt Control* 2000; 122: 210–215.
92. Artemis Intelligent Power Ltd. Digital displacement hybrid transmissions, http://www.artemisip.com/appli_auto_transm.htm (2008, accessed 7 August 2009).
93. Achten PAJ. The hybrid transmission. SAE paper 2007-01-4152, 2007.
94. Achten PAJ. Variable hydraulic transformer. *Des News* 2002; 58: 48.
95. Hitchcox AL. Floating cups instead of pistons. *Hydraulics Pneumatics* 2006; September: 16–17.
96. Wu B, Lin C-C, Filipi Z, et al. Optimal power management for a hydraulic hybrid delivery truck. *Veh System Dynamics* 2004; 42: 23–40.

97. Hall R and Kargul JJ. Hydraulic hybrid promises big savings for UPS. *Hydraulics Pneumatics* 2006; 59: 42–45.
98. Filipi Z, Louca L, Daran B, et al. Combined optimisation of design and power management of the hydraulic hybrid propulsion system for the 6×6 medium truck. *Int J Heavy Vehicle Systems* 2004; 11: 372–402.
99. Toulson ER. Evaluation of a hybrid hydraulic launch assist system for use in small road vehicles. In: *IEEE international symposium on industrial electronics*, Cambridge, UK, 30 June–2 July 2008, pp.967–972. New York: IEEE.
100. Wicks F, Maleszewski J, Wright C and Zarybnicky J. Analysis of compressed air regenerative braking and a thermally enhanced option. In: *37th intersociety energy conversion engineering conference*, Washington, DC, USA, 29–31 July 2004, pp.406–411. New York: IEEE.
101. Tata Motors Ltd. An engine which uses air as fuel, <http://www.tatamotors.com/media/press-releases.php?id=281> (2009, accessed 9 August 2009).
102. Midgley WJB and Cebon D. Architecture of regenerative braking systems for heavy goods vehicles. In: *10th international symposium on advanced vehicle control*, Loughborough, UK, 22–26 August 2010, vol. 10, paper no. 192. Tokyo: Japan Society of Automotive Engineers.
103. *MF08–MFE08 hydrobases – technical catalog*. Verboric: Poclairn Hydraulics, 2008.

Appendix

Notation

a_d	demanded acceleration	E_t	energy storage of the total system
C	capacitance	E_u	energy storage of an ultra-capacitor
e_b	specific energy of a battery	E_v^0	initial kinetic energy of the vehicle
e_t	specific energy of the total system	\dot{E}_a	power of an actuator
e_u	specific energy of an ultra-capacitor	\dot{E}_{acc}	power of an accumulator
\dot{e}_a	specific power of an actuator	\dot{E}_{avg}	average power of an accumulator
\dot{e}_s	specific power of energy storage	\dot{E}_{max}	maximum power
\dot{e}_t	specific power of the total system	\dot{E}_s	power of energy storage
\dot{e}_u	specific power of an ultra-capacitor	\dot{E}_t	power of the total system
\tilde{e}_s	volumetric energy of energy storage	\dot{E}_u	power of an ultra-capacitor
\tilde{e}_t	volumetric energy of the total system	g	acceleration due to gravity
\tilde{e}_a	volumetric power of an actuator	J	rotational inertia
\tilde{e}_t	volumetric power of the total system	m_a	mass of an actuator
E_{acc}	energy storage of an accumulator	m_b	mass of a battery
E_b	energy storage of a battery	m_s	total mass of energy storage
E_f	energy storage of a flywheel	m_t	mass of the total system
		$m_{t,e}$	mass of the total system when specified to meet the energy requirement
		$m_{t,p}$	mass of the total system when specified to meet the power requirement
		m_u	mass of an ultra-capacitor
		m_v	mass of the vehicle
		P	pressure
		P_{atm}	atmospheric pressure
		P_{comp}	pressure in the compressed state
		P_{max}	maximum pressure
		P_{min}	minimum pressure
		Q	flow rate
		Q_{avg}	average flow rate
		Q_{max}	maximum flow rate
		r_p	pressure ratio
		r_v	volume ratio
		R	radius
		U	stored energy
		v_i	initial velocity
		v_{comp}	volume in the compressed state
		V	voltage
		x	ratio of the ultra-capacitor energy storage to the battery energy storage
		γ	adiabatic index
		ρ	density
		σ_f	fracture stress
		ω	rotational speed
		ω_{max}	maximum rotational speed